



“The **more** opportunities there are to get **students involved**, the more you will **encourage** previously unreached and **unrepresented groups** to join the Earth and Space science community.”

Ryan Haupt

Research Fellow,
Smithsonian Museum
of Natural History
2015 Student Travel
Grant Recipient

Support the next generation of Earth and space scientists.
Donate to the Austin Student Travel Grant Challenge.

AGU100 ADVANCING
EARTH AND
SPACE SCIENCE

agu.org/austin | [#AGU100](https://twitter.com/AGU100)

Geophysical Research Letters

RESEARCH LETTER

10.1029/2018GL081355

Key Points:

- We report the first seasonal changes of the upper surface dissolved iron concentrations of four occupations from late winter to late summer
- Euphotic zone dissolved iron decreases due to biological uptake, while aphotic iron decreases due to colloidal aggregation and scavenging
- Recycling of nutrients might be responsible for sustaining the observed seasonal primary production in late January to early February

Supporting Information:

- Supporting Information S1

Correspondence to:

T. N. Mtshali,
tmtshali@csir.co.za

Citation:

Mtshali, T. N., van Horsten, N. R., Thomalla, S. J., Ryan-Keogh, T. J., Nicholson, S.-A., Roychoudhury, A. N., et al. (2019). Seasonal depletion of the dissolved iron reservoirs in the sub-Antarctic Zone of the Southern Atlantic Ocean. *Geophysical Research Letters*, 46, 4386–4395. <https://doi.org/10.1029/2018GL081355>











Received 21 NOV 2018

Accepted 5 APR 2019

Accepted article online 8 APR 2019

Published online 30 APR 2019

Seasonal Depletion of the Dissolved Iron Reservoirs in the Sub-Antarctic Zone of the Southern Atlantic Ocean

T. N. Mtshali¹ , N. R. van Horsten^{1,2,3} , S. J. Thomalla¹ , T. J. Ryan-Keogh¹ , S.-A. Nicholson¹ , A. N. Roychoudhury² , E. Bucciarelli³ , G. Sarthou³ , A. Tagliabue⁴ , and P. M. S. Monteiro¹ 

¹Southern Ocean Carbon and Climate Observatory, Natural Resources and Environment, CSIR, Cape Town, South Africa,

²Department of Earth Sciences, Stellenbosch University, Stellenbosch, South Africa, ³CNRS, Univ. Brest, IRD, Ifremer, Laboratoire des Sciences de l'environnement marin, Technopôle Brest-Iroise, Plouzané, France, ⁴Department of Earth, Ocean and Ecological Sciences, School of Environmental Sciences, University of Liverpool, Liverpool, UK

Abstract Seasonal progression of dissolved iron (DFe) concentrations in the upper water column was examined during four occupations in the Atlantic sector of the Southern Ocean. DFe inventories from euphotic and aphotic reservoirs decreased progressively from July to February, while dissolved inorganic nitrogen decreased from July to January with no significant change between January and February. Results suggest that between July and January, DFe loss from both euphotic and aphotic reservoirs was predominantly in support of phytoplankton growth (iron-to-carbon uptake ratio of $16 \pm 3 \mu\text{mol/mol}$), highlighting the importance of the “winter DFe reservoir” for biological uptake. During January to February, excess loss of DFe relative to dissolved inorganic nitrogen (iron-to-carbon uptake ratio of $44 \pm 8 \mu\text{mol/mol}$ and aphotic DFe loss rate of $0.34 \pm 0.06 \mu\text{mol}\cdot\text{m}^{-2}\cdot\text{day}^{-1}$) suggests that scavenging is the dominant removal mechanism of DFe from the aphotic, while continued production is likely supported by recycled nutrients.

Plain Language Summary Trace metal iron is one of the limiting nutrients for primary productivity in the Southern Ocean; however, the relative importance of seasonal iron supply and sinks remains poorly understood, due to sparse data coverage across the seasonal cycle and lack of high-resolution dissolved iron (DFe) measurements. Here we present four “snapshots” of DFe measurements at a single station in the southeast Southern Atlantic Ocean (one in winter and three in late spring-summer), to address the seasonal evolution of DFe and dissolved inorganic nitrogen (DIN) concentrations within the biologically active sunlit and subsurface reservoirs. We observed a seasonal depletion of DFe inventories from July to February, while DIN inventories decrease from July to January with no concomitant changes between January and February. This suggests that in addition to biological uptake in the sunlit layer, the observed decrease in DFe inventories below this (relative to DIN) is driven by aggregation and incorporation of iron particles into larger “marine snow” sinking particles, while nutrient recycling is driving the observed continuation of primary productivity during late summer. Our results provide insight into seasonal change of DFe availability in different reservoirs where interplay between removal and supply processes are controlling its distributions and bioavailability to support upper surface primary production.

1. Introduction

Iron availability in the Southern Ocean (SO) controls phytoplankton growth, plankton community composition, and carbon export to the deep ocean through the biological carbon pump (Tagliabue et al., 2014). Although the spatial distribution of SO blooms is known to be driven by iron availability (Pollard et al., 2009), different seasonal expressions of these blooms, with both high and low seasonal cycle reproducibility, implies distinct regulatory supply mechanisms (Thomalla et al., 2011). Indeed, variability in iron supply can significantly impact maximum potential primary production (PP) across the SO (by as much as 80%; Ryan-Keogh et al., 2017). The iron supply across the seasonal cycle can be divided into three terms: new supply, recycled supply, and internal transport (Boyd & Ellwood, 2010; Boyd, Ibsanmi, et al., 2010). The processes and sources responsible for these different supply mechanisms include, but are not limited to, deep winter mixing (Tagliabue et al., 2014), internal metal transformations (Boyd, Strzepak, et al., 2010; Boyd et al., 2017), aerosols (Jickells et al., 2005), sediments (Planquette et al., 2007), sea ice and icebergs (Lancelot

et al., 2009), hydrothermal vents (Tagliabue et al., 2010), upwelling (Klunder et al., 2011), eddy diffusion (Law et al., 2003), and horizontal and lateral advection (Chever, Sarthou, et al., 2010). The relative importance of iron supply pathways remains poorly understood, primarily due to sparse data coverage across the seasonal cycle in the SO (Tagliabue et al., 2012). This hampers our ability to constrain the response of the biological carbon pump to climate change in this key region of the world's oceans. A compilation study of dissolved iron (DFe) measurements concluded that even in regions where many DFe measurements exist, the processes governing the seasonal evolution remain poorly constrained, which suggests that biological consumption may not be the major driver of DFe variability (Tagliabue et al., 2012). The number of in situ DFe measurements available for the Global Ocean is rapidly increasing, thanks to efforts made by programs such as GEOTRACES (Intermediate Data Products; Schlitzer et al., 2018; Mawji et al., 2015). Nonetheless, missing measurements during key seasonal transitions make it difficult to quantify and understand surface water replenishment processes and the seasonal DFe cycle, especially in the SO (Tagliabue et al., 2012).

Phytoplankton blooms in the sub-Antarctic Zone (SAZ) of the SO are characterized by high interannual and intraseasonal variability with an extended duration (e.g., ~16 weeks in Racault et al., 2012) that sustains high chlorophyll concentrations late into summer (Carranza & Gille, 2015; Swart et al., 2015; Thomalla et al., 2011, 2015). The longevity of these blooms is unusual as DFe limitation at this time of year is expected to limit growth (Boyd & Doney, 2002). Deep winter mixing entrains DFe and macronutrients from subsurface reservoirs, replenishing the mixed layer to support springtime PP. However, upper ocean biota and abiotic scavenging onto settling particles rapidly depletes this mixed layer inventory (Tagliabue et al., 2012, 2014). Although diapycnal diffusion resupplies the mixed layer from late spring onward, its low rates cannot be reconciled with phytoplankton utilization. Instead, summertime blooms are sustained by this "once-off" winter entrainment supply of nutrients through biologically mediated recycling (Boyd et al., 2012, 2017; Strzepek et al., 2005; Tagliabue et al., 2014). However, there is now growing evidence to suggest that in addition to the entrained supply, intermittent storm-driven mixing may also play a role in extending the duration of summertime production through intraseasonal entrainment of DFe from a subsurface reservoir beneath the productive layer (Carranza & Gille, 2015; Fauchereau et al., 2011; Nicholson et al., 2016; Swart et al., 2015; Thomalla et al., 2011).

SO phytoplankton species can display a large degree of plasticity in their elemental stoichiometry, as opposed to previous theory of canonical Redfield ratios. This is best demonstrated by the 100-fold difference measured in Fe-to-carbon (Fe:C) ratios from both in situ and laboratory studies (ranging 0.29–25.00 $\mu\text{mol/mol}$; Abraham et al., 2000; Fung et al., 2000; Sarthou et al., 2008; Strzepek et al., 2011, 2012; Twining, Baines, & Fisher, 2004; Twining, Baines, Fisher, & Landry, 2004), which is a function of cell size, light, and DFe availability (Sunda & Huntsman, 1997; Geider & La Roche, 2002). Overall changes in DFe include Fe-specific losses such as scavenging and colloidal aggregation (which could be captured by total or particulate Fe measurements), such that seasonal changes in Fe:C ratios and their comparison to known algal demands can be used to enhance our understanding of the drivers of variability. This paper aims to understand the seasonal progression of DFe concentrations in the upper 200 m of the water column by examining changes in stoichiometry and nutrient inventories from different depth horizons at a single location in the SAZ of the south Atlantic SO.

2. Materials and Methods

Data presented here were obtained during two cruises on board the SA Agulhas II in winter (22 July to 15 August 2015) and summer (3 December 2015 to 11 February 2016) as part of SOSCEX III (Swart et al., 2012). Results focus on a process station within the SAZ (Figure 1a), which was sampled on 28 July 2015, 8 December 2015, 5 January 2016, and 8 February 2016, while a Seaglider deployed in July (at 42.7°S, 8.7°E) in mooring mode sampled continuously for ~6 months for potential temperature, salinity, and fluorescence-derived chlorophyll and retrieved in February (at 43.0°S, 8.5°E; supporting information Figure S1).

Full methodology is presented in supporting information Text S1. Briefly, following a GEOTRACES sampling protocol (Cutter et al., 2013), acidified DFe samples were analyzed using flow injection analysis with chemiluminescence detection (Obata et al., 1993; Sarthou et al., 2003). Dissolved inorganic nitrogen (nitrate + nitrite; DIN) samples were measured using a Lachat flow injection analysis (Egan, 2008; Wolters, 2002). The mixed layer depth (MLD) was defined as the depth where density differs from surface (10 m) density by more than 0.03 kg/m^3 (de Boyer Montégut et al., 2004). The euphotic depth (Z_{eu}) was

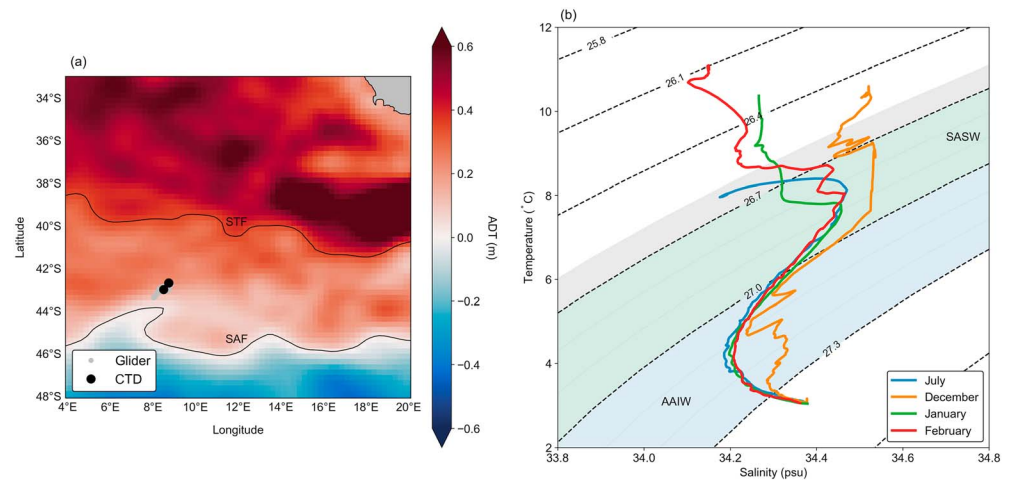


Figure 1. Map of (a) absolute dynamic topography (ADT, m) showing process station location and glider position, with the position of subtropical front (STF) and sub-Antarctic front (SAF) as determined by maps of ADT gradients (Swart et al., 2010) from the CLS-AVISO product (Rio et al., 2011); and (b) temperature-salinity plot made from colocated (temporally and spatially) glider profiles (0–1,000 m) from each occupancy indicating the presence of Antarctic intermediate water (AAIW) and sub-Antarctic surface water (SASW). CTD = conductivity-temperature-depth.

defined as the depth at which photosynthetically active radiation (PAR) is 1% of the surface value. The isopycnal depth of deep winter mixing was identified at a density threshold of 26.70 kg/m^3 and extended throughout summer to represent remnant winter waters. Depth-integrated PP rates (PP_{wc} , $\text{mol C}\cdot\text{m}^{-2}\cdot\text{day}^{-1}$) were calculated from quenching corrected glider-derived chlorophyll (Thomalla, Moutier, et al., 2017) and PAR according to Platt et al. (1980), Platt and Sathyendranath (1993), and Thomalla et al. (2015). PP parameters were determined from a linear relationship with chlorophyll using experimental values from both cruises (supporting information Figure S2; Ryan-Ryan-Keogh, Thomalla, Little, et al., 2018). Seasonal variation in nutrient concentrations within the euphotic and winter mixed layer isopycnals required three different methods to derive depth-integrated nutrient inventories. Significant differences were calculated using a *t* test of two samples assuming equal variance and one-way analysis of variance (ANOVA) single factor, with significant results reported at the 95% confidence level.

3. Results

3.1. Station Characterization

3.1.1. Hydrographic Context

Sea surface temperatures ranged from 7.0 to 10.8 °C with salinity ranging from 34.1 to 34.6. Surface chlorophyll concentrations were low ($\sim 0.28 \mu\text{g/L}$) throughout winter (July–October), increasing to a maximum of 1.40 $\mu\text{g/L}$ in December (supporting information Figure S1c). The deepest MLD from the glider data set was observed in October (169 m) compared to July (157 m), suggesting that July does not correspond to the timing of deepest winter convective mixing. Seasonal heating of the upper water column in summer (December–February) resulted in a shoaling of the MLD to a 16- to 43-m range. The extended isopycnal depth of the deepest winter mixed layer during summer ranged from 131 to 149 m, which was 89–119 m deeper than the summer MLD. Z_{eu} did not vary significantly, with a mean value of 63 ± 7 m. Although the station has the same geographical location, it is also positioned within the larger eastward flowing Antarctic Circumpolar Current. Thus, the water sampled during each occupation will be slightly different as the water is advected eastward. Nevertheless, the water mass characterization (Figure 1b) between each occupancy is relatively consistent. However, the December occupation exhibited a temperature-salinity signature of warmer (>9.0 °C), saltier (>34.5) subtropical water (Boye et al., 2012; Chever, Bucciarelli, et al., 2010; Joubert et al., 2011), suggesting an intrusion of Agulhas water. Due to the distinct water mass sampled in December, calculated nutrient inventories do not form part of the budget calculations; profiles are nonetheless included to explore seasonal changes in nutrient inventories.

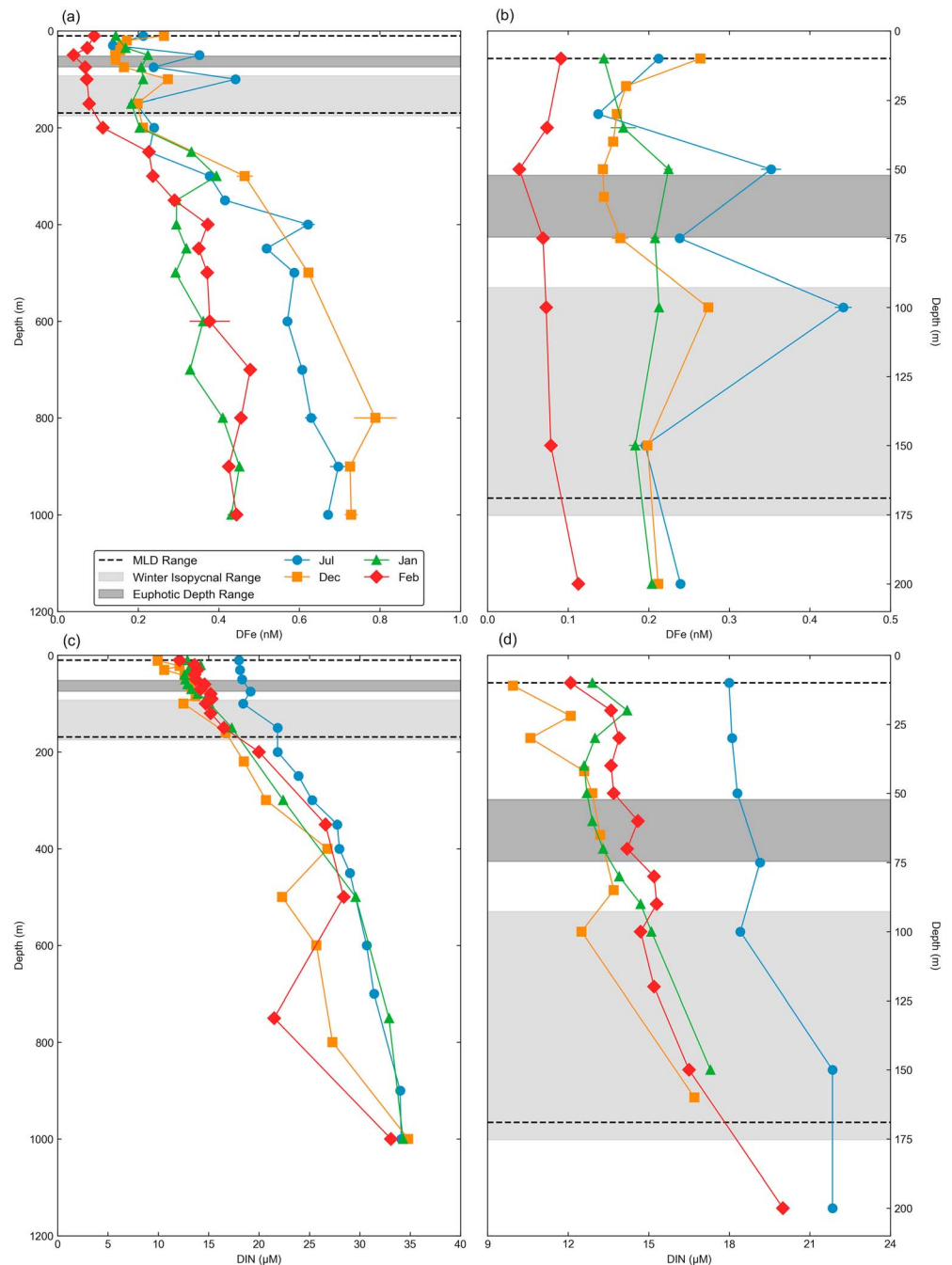


Figure 2. Vertical profiles of (a) dissolved iron (DFe, nM) with \pm standard deviation, (b) insert of upper water column DFe concentrations, (c) vertical profiles of dissolved inorganic nitrogen (DIN, μ M), and (d) insert of upper water column DIN concentrations. MLD = mixed layer depth.

3.1.2. Vertical Profiles of DFe and DIN Concentrations

DFe concentrations in July ranged between 0.14 and 0.70 nM, with two pronounced peaks above the isopycnal layer of winter and summer MLD (50 m = 0.35 ± 0.01 nM and 100 m = 0.44 ± 0.01 nM; Figures 2a and 2b). During December and February, DFe concentrations showed a slight elevation in near surface waters, decreasing to minimum values in the subsurface, followed by increasing concentrations with depth, while concentrations in January increased with depth. December concentrations ranged between 0.14 and 0.79 nM, with a peak at 100 m (0.27 ± 0.00 nM), while in January and February, concentrations ranged between 0.14 and 0.45 and 0.04 and 0.48 nM, respectively. DFe profiles displayed two distinct features: (i)

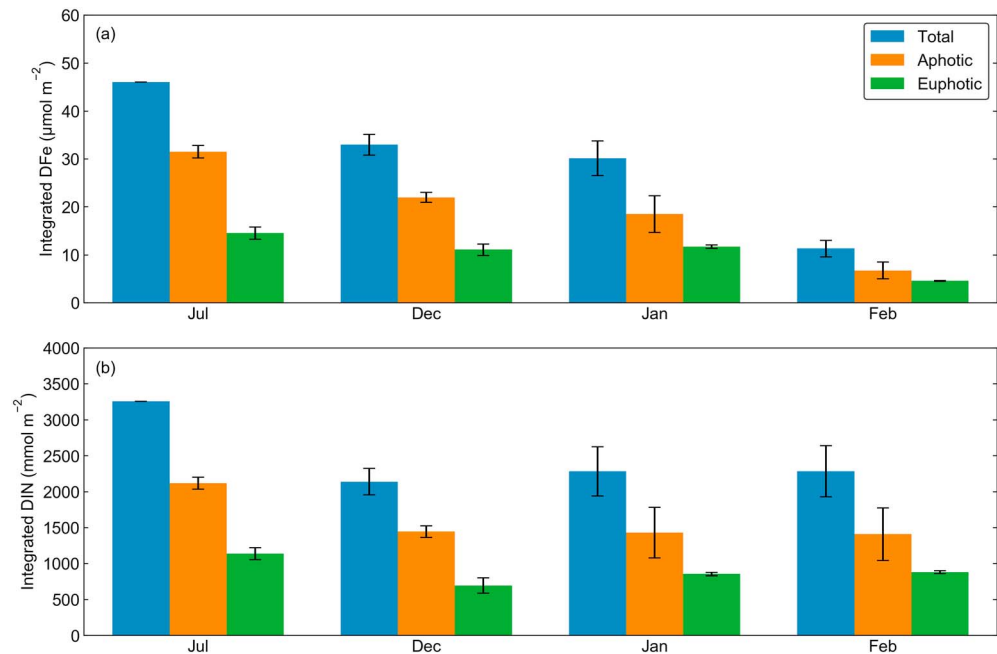


Figure 3. Plots of the mean depth-integrated (a) dissolved iron (DFe, $\mu\text{mol}/\text{m}^2$) and (b) dissolved inorganic nitrogen (DIN, mmol/m^2) inventories with \pm standard deviations, between total, aphotic, and euphotic reservoirs.

variability in deep water concentrations (elevated in July and December and lower in January and February) that is largely influenced by inflow of different water masses into the SAZ (Boye et al., 2012; Klunder et al., 2011; Piola & Gordon, 1989) and (ii) upper water column (<200 m) concentrations that were elevated in July and depleted in February. DIN profiles typically showed minimum concentrations at the surface increasing with depth (Figure 2c), with higher surface concentrations in winter than in summer, decreasing from 18.0 μM in July to 10.0 μM in December, followed by slight increases to 12.9 and 12.1 μM in January and February, respectively (Figure 2d).

3.2. Depth-Integrated DFe Inventories

DFe concentrations in the upper water column were binned into two inventories: the euphotic (integrated from surface to Z_{eu}) and aphotic inventories (integrated from Z_{eu} to depth of the winter isopycnal layer), with the total upper water column inventory being the sum of these two reservoirs (supporting information Table S1). DFe inventories were significantly lower throughout summer relative to winter across all depth horizons (Figure 3a, ANOVA, $p < 0.05$). Between July and February, total upper water column DFe inventories decreased from 46 ± 0 to $11 \pm 2 \mu\text{mol}/\text{m}^2$. A similar trend was observed within the euphotic and aphotic reservoirs, which decreased from 14 ± 1 to $5 \pm 0.1 \mu\text{mol}/\text{m}^2$ and from 32 ± 1 to $7 \pm 2 \mu\text{mol}/\text{m}^2$, respectively. A decrease in the total upper water column inventory resulted in a DFe loss of $35 \pm 2 \mu\text{mol}/\text{m}^2$, of which $\sim 71\%$ was from the aphotic reservoir. Between July and January, the observed decrease in euphotic and aphotic inventories resulted in DFe losses of 3 ± 1 and $13 \pm 5 \mu\text{mol}/\text{m}^2$, which equates to loss rates of 0.02 ± 0.01 and $0.08 \pm 0.03 \mu\text{mol}\cdot\text{m}^{-2}\cdot\text{day}^{-1}$, respectively. From January to February, both euphotic and aphotic DFe losses were 7 ± 0.3 and $12 \pm 2 \mu\text{mol}/\text{m}^2$ with loss rates of 0.20 ± 0.01 and $0.34 \pm 0.06 \mu\text{mol}\cdot\text{m}^{-2}\cdot\text{day}^{-1}$.

3.3. Depth-Integrated DIN Inventories

Unlike the trends observed for DFe, DIN inventories decreased from July to January with no significant changes observed between January and February across all depth horizons (supporting information Table S1 and Figure 3b, ANOVA, $p > 0.05$). Another notable difference is that total upper water column inventories of DIN in December were lower than those in January and February, indicative of the intrusion of low macronutrient subtropical water. Henceforth, this month is excluded from budget calculations. Between July and January, the observed euphotic and aphotic DIN losses were $283 \pm 90 \text{mmol}/\text{m}^2$ (loss rate

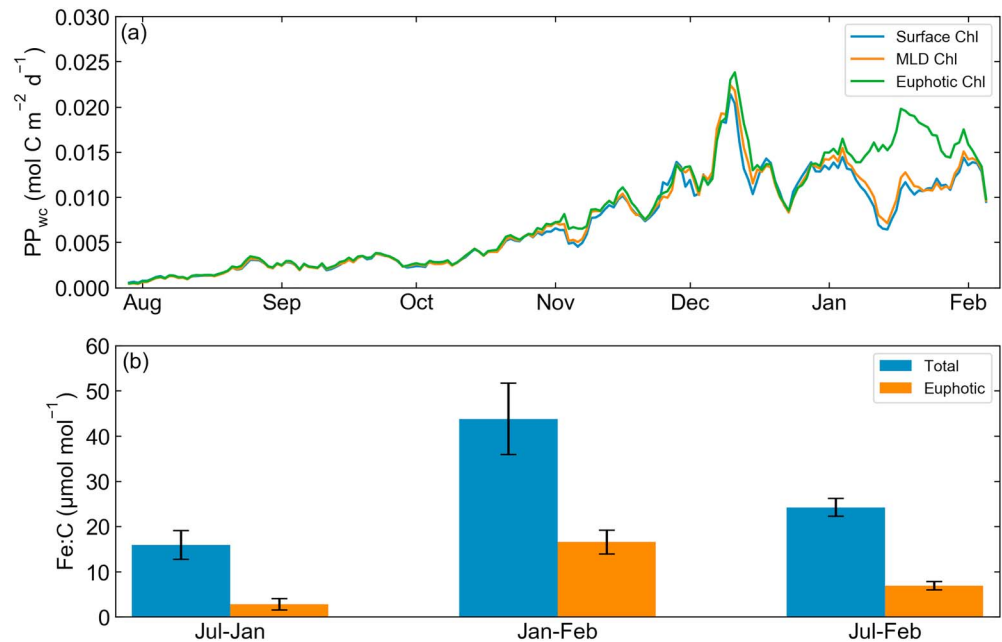


Figure 4. Plots of (a) the time series of PP_{wc} derived from glider chlorophyll concentrations from the surface, mixed layer (MLD), and euphotic zone ($\text{mol C}\cdot\text{m}^{-2}\cdot\text{day}^{-1}$) and (b) estimates of Fe:C ratios ($\mu\text{mol/mol}$) for total and euphotic reservoirs over the season.

of $1.8 \pm 0.6 \text{ mmol}\cdot\text{m}^{-2}\cdot\text{day}^{-1}$) and $689 \pm 431 \text{ mmol/m}^2$ (loss rate of $4 \pm 3 \text{ mmol}\cdot\text{m}^{-2}\cdot\text{day}^{-1}$), respectively, while between January and February there was euphotic accumulation of $24 \pm 0.8 \text{ mmol/m}^2$ and aphotic loss of $22 \pm 14 \text{ mmol/m}^2$. A similar seasonal decrease was observed in DIN inventories, and again, $\sim 73\%$ of the total upper water column loss could be accounted for from the aphotic layer.

3.4. Primary Productivity Estimates and Iron-to-Carbon Ratios

Mean PP_{wc} rates (Figure 4a) were low between July and October ($2.1 \pm 0.05 \text{ mmol C}\cdot\text{m}^{-2}\cdot\text{day}^{-1}$) alongside deep MLD and low average light intensity (mean MLD and PAR are 119.1 m and $480.4 \mu\text{mol photons}\cdot\text{m}^{-2}\cdot\text{s}^{-1}$, respectively; supporting information Figure S3). Between October and January the MLD shoaled and light availability increased (mean MLD and PAR are 71.6 m and $708.8 \mu\text{mol photons}\cdot\text{m}^{-2}\cdot\text{s}^{-1}$, respectively), driving increased mean PP_{wc} ($10.5 \pm 0.2 \text{ mmol C}\cdot\text{m}^{-2}\cdot\text{day}^{-1}$) that reached maximum between December and January, remaining similar between January and February ($12.3 \pm 2.1 \text{ mmol C}\cdot\text{m}^{-2}\cdot\text{day}^{-1}$). Phytoplankton Fe:C uptake ratios were calculated based upon the DFe loss between occupations and the cumulative sum of carbon gained via PP_{wc} (corrected for the number of days between occupations; Figure 4b and supporting information Table S1). Between July and January, the total upper water column Fe:C ratio was $16 \pm 3 \mu\text{mol/mol}$, with a euphotic ratio of $3 \pm 1 \mu\text{mol/mol}$, whereas between January and February, the total upper water column ratio was $44 \pm 8 \mu\text{mol/mol}$, with a euphotic ratio of $17 \pm 3 \mu\text{mol/mol}$. Between July and February, the total upper water column ratio was $24 \pm 2 \mu\text{mol/mol}$, with a euphotic ratio of $7 \pm 1 \mu\text{mol/mol}$.

4. Discussion

The importance of iron in the SO is well established; however, the relative importance of seasonal iron supply and removal pathways remains poorly understood. This is primarily due to sparse data coverage across the seasonal cycle and a lack of high-resolution DFe profiles, which limits our understanding of seasonal drivers of upper ocean Fe supply (Tagliabue et al., 2012). In this study, the seasonal progression of DFe concentrations at four occupations in the SAZ (spanning multiple seasons from winter through to late summer) was examined to understand processes that control DFe supply/removal and demand. Vertical DFe concentrations were typically $<1.0 \text{ nM}$, with lower surface concentrations that increased with depth (Figure 2a). The winter profile was different from summer in that DFe concentrations were elevated within the MLD

(Figure 2b), suggesting typical winter DFe supply from a deep water source (Ellwood et al., 2008; Sohrin et al., 2000). To our knowledge, there is only one other winter DFe data set reported for the Indian sector of the SO (Ellwood et al., 2008), where winter values were significantly lower (42.27°S, 159.99°E; range: 0.08–0.41 nM, upper 500 m; $p < 0.05$), highlighting differences in DFe concentration between ocean basins (Tagliabue et al., 2012). DFe concentrations in summer, particularly in February, are in good agreement with previous values reported for the SAZ (Chever, Bucciarelli, et al., 2010, range: 0.09–0.44 nM upper 1,029 m; Klunder et al., 2011, range: 0.18–0.46 nM upper 1,253 m; Abadie et al., 2017, range: 0.09–0.60 nM upper 1,468 m). The observed seasonal changes in nutrient availability within the total upper water column and the distribution of nutrient inventories within different depth horizons were used to investigate possible supply and removal processes responsible for observed seasonal variability.

Depth-integrated nutrient inventories from all depth horizons show that both DFe and DIN in July were high, due to deep winter mixing (Figures 3a and 3b). Between July and February, both DFe and DIN inventories in the total upper water column showed a substantial decrease that was driven mainly by losses from the aphotic layer (~70%), suggesting losses through a combination of vertical supply of both nutrients (through rapid recycling) in support of surface production, bacterial uptake and/or DIN losses through denitrification, and iron losses through scavenging. The added value of multiple occupations, however, becomes clear when changes in inventories are investigated during interim occupations (i.e., between July and January), when both nutrient inventories decrease, compared to between January and February, when little change is observed in DIN, but DFe is depleted in all inventories.

Focusing on changes in the euphotic nutrient inventory losses during the winter–early summer transition (July to January) results in a DFe:DIN loss ratio of $9 \pm 2 \mu\text{mol/mol}$, which when assuming a Redfield C:N ratio of 6.6 equates to an Fe:C uptake ratio of $1.4 \pm 0.4 \mu\text{mol/mol}$, which is similar to the euphotic-zone PP-estimated Fe:C ratio of $2.8 \pm 1 \mu\text{mol/mol}$. Assuming an average Chl:C ratio of 0.02 mg Chl/mg C (Thomalla, Ogunkoya, et al., 2017) and converting and integrating the colocated glider-derived chlorophyll into phytoplankton carbon (C_{phyto}), the calculated euphotic Fe:C ratio of $0.4 \pm 0.2 \mu\text{mol/mol}$ is lower than the estimated ratios above (supporting information Figures S4 and S5 and Table S3). However, all of these values agree well with ratios reported in the literature (mean = $4.6 \pm 4.6 \mu\text{mol/mol}$, range: 0.29–25.00; supporting information Table S2). Furthermore, within the total upper water column, the estimated Fe:C ratio ($16 \pm 3 \mu\text{mol/mol}$) from PP falls within the range reported in the literature, suggesting that the observed DFe loss (from “winter reserve stock”) during the first half of the growing season is predominantly in support of phytoplankton growth. However, since the ratio falls above the mean literature value, other loss processes (i.e., scavenging) may also be at play.

In contrast, progressing further into late summer (January to February), a continual decrease in DFe inventories from both reservoirs was observed, with little change observed in DIN, despite continued PP (Figures 3a and 3b). An absence of change in DIN inventories suggests a resupply of DIN through remineralization processes, which would imply a similar DFe supply, to sustain the observed production (Bowie et al., 2001; Boyd et al., 2017). Although Fe:C uptake ratios of $17 \pm 3 \mu\text{mol/mol}$ from the euphotic zone fall within the reported literature range, loss from the total upper water column results in an Fe:C ratio of $44 \pm 8 \mu\text{mol/mol}$, which is outside the likely range of biological uptake in the presence of only 0.1- to 0.2-nM DFe concentrations. These results suggest that in addition to biological Fe consumption within the euphotic zone, colloidal Fe aggregation and scavenging onto sinking particles are most likely driving the observed loss of DFe from the aphotic. To examine if colloidal aggregation and scavenging are the primary loss mechanisms between January and February, aphotic DFe loss rates were used as a proxy for scavenging, in the absence of particulate iron flux rates. The observed euphotic and aphotic DFe loss rates of 0.20 ± 0.01 and $0.34 \pm 0.06 \mu\text{mol}\cdot\text{m}^{-2}\cdot\text{day}^{-1}$, respectively, are consistent with other scavenging rates that are better defined by downward particulate iron export fluxes (Bowie et al., 2009, 0.17 ± 0.09 and $0.21 \pm 0.05 \mu\text{mol}\cdot\text{m}^{-2}\cdot\text{day}^{-1}$ at mixed layers 53 and 70 m, respectively; Frew et al., 2006, 0.22 ± 0.03 and $0.55 \pm 0.06 \mu\text{mol}\cdot\text{m}^{-2}\cdot\text{day}^{-1}$ at mixed layers 80 and 120 m, respectively). Furthermore, the total upper water column Fe:C loss ratio is consistent with previously reported Fe:C export ratios (given the significant ranges) in the SAZ from sediment traps (Bowie et al., 2009, 50 ± 38 to $248 \pm 125 \mu\text{mol/mol}$; Frew et al., 2006, 167–218 $\mu\text{mol/mol}$). It should be noted, however, that these Fe:C export ratios will include a lithogenic component and as such are expected to be higher than our estimated uptake ratios.

Overall, estimated Fe:C uptake ratios and DFe loss rates seem to agree that the dominant loss process for Fe in early summer (July–January) within the euphotic and total upper water column is most likely driven by biological uptake, in comparison to late summer (January–February) where the dominant processes are both biological consumption in the euphotic zone and scavenging in the aphotic zone. The lack of change in DIN and depletion of DFe inventories during late summer combined with continual growth suggest that the system is supported by rapidly recycled nutrients, in accordance with previous studies (Bowie et al., 2001; Boyd et al., 2012, 2017, 2005; Strzepek et al., 2005; Tagliabue et al., 2014). However, the observed emergence of a distinct subsurface bloom below the mixed layer that persists throughout January (supporting information Figure S1c) implies an insufficient DFe supply within the mixed layer to sustain phytoplankton growth. These findings are corroborated by concurrent iron addition incubation experiments from the mixed layer (Ryan-Keogh, Thomalla, Mtshali, et al., 2018), which show maximum increases in photosynthetic efficiency and net chlorophyll growth rates following iron addition in January and February, compared to December (no response). A transient MLD deepening event in February that was linked to an increase in wind stress (Ryan-Keogh, Thomalla, Mtshali, et al., 2018) led to a subsequent increase in phytoplankton biomass throughout the MLD (supporting information Figure S1c), suggesting that storms may nonetheless play a role in entraining subsurface DFe and DIN in support of surface water production utilizing regenerated nitrogen (Nicholson et al., 2016, Ryan-Keogh, Thomalla, Mtshali, et al., 2018). Unfortunately, monthly-scale sampling of DFe profiles is insufficient to capture specific synoptic events that contribute to the seasonal progression of DFe supply and removal, for example, (i) the intrusion of subtropical waters linked to Agulhas eddies in the SAZ, which can deliver Fe-rich, low-macronutrient waters (Chever, Bucciarelli, et al., 2010), and (ii) wind-induced mixed layer deepening events (e.g., in early February). Future studies must therefore sample at a greater frequency in line with the time scales of these synoptic events, in order to better capture the full range of seasonal drivers of Fe-pool supply and demand.

5. Summary

This study examined the seasonal evolution of DFe relative to DIN within the upper water column, exploring different mechanisms driving seasonal changes in DFe. This was achieved through seasonal-scale observations of DFe profiles at a single station located in the SAZ of the south Atlantic SO. Results show a progressive seasonal decrease in DFe inventories from July to February in all depth horizons, while DIN decreases from July to January with no significant change from January to February. During late summer (January to February), a temporal decrease of DFe within both euphotic and aphotic reservoirs relative to DIN inventories suggests that the processes that drive DFe loss are Fe specific. We propose the following: (i) In July, deep convective mixing replenishes the mixed layer driving high Fe inventories. (ii) This total upper water column reservoir (both euphotic and aphotic) declines between July and January, due to biological Fe consumption in support of phytoplankton growth (supported by Fe:C uptake ratios that fall within the reported literature range). (iii) During late summer (January to February), in addition to biological uptake in the euphotic layer, the high Fe:C uptake ratio within the total upper water column and the observed euphotic and aphotic zone DFe loss rates suggests that aggregation of colloidal Fe and scavenging onto settling particles are the dominant drivers of the observed Fe signal, with PP in the euphotic layer likely supported by recycling and possible event-scale entrainment of nutrients.

References

- Abadie, C., Lacan, F., Radic, A., Pradoux, C., & Poitrasson, F. (2017). Iron isotopes reveal distinct dissolved iron sources and pathways in the intermediate versus deep Southern Ocean. *Proceedings of the National Academy of Sciences*, *114*, 858–863. <https://doi.org/10.1073/pnas.1603107114>
- Abraham, E. R., Law, C. S., Boyd, P. W., Lavender, S. J., Maldonado, M. T., & Bowie, A. R. (2000). Importance of stirring in the development of an iron-fertilized phytoplankton bloom. *Nature*, *407*, 727. <https://doi.org/10.1038/35037555>
- Bowie, A. R., Lannuzel, D., Remenyi, T. A., Wagener, T., Lam, P. J., Boyd, P. W., et al. (2009). Biogeochemical iron budget of the Southern Ocean south of Australia: Decoupling of iron and nutrient cycles in the subantarctic zone by summertime supply. *Global Biogeochemical Cycles*, *23*, GB4034. <https://doi.org/10.1029/2009GB003500>
- Bowie, A. W., Maldonado, M. T., Frew, R. D., Croot, P. L., Achterberg, E. P., Mantoura, F. C., et al. (2001). The fate of added iron during a mesoscale fertilization experiment in the Southern Ocean. *Deep-Sea Research II*, *48*, 2703–2743. [https://doi.org/10.1016/S0967-0645\(01\)00015-7](https://doi.org/10.1016/S0967-0645(01)00015-7)
- Boyd, P. W., Arrigo, K. R., Strzepek, R., & van Dijken, G. L. (2012). Mapping phytoplankton iron utilization: Insights into Southern Ocean supply mechanisms. *Journal of Geophysical Research*, *117*, C06009. <https://doi.org/10.1029/2011JC007726>

Acknowledgments

We would like to thank the South African National Antarctic Programme (SANAP) and the captain, crew of the SA Agulhas II, and all the students who helped us collect samples and for their professional support throughout the cruises. We would also like to thank the Editor and two anonymous reviewers for constructive criticism. This was undertaken and supported through CSIR's Southern Ocean Carbon and Climate Observatory (SOCCO) Programme (<http://socco.org.za/>) funded by the Department of Science and Technology. This work was supported by CSIR's Parliamentary Grant funding (SNA2011112600001) and the NRF SANAP grants SNA14073184298 to T. N. M. and SNA14070974732 to A. N. R. N. R. v. H. was funded by ICEMASA Mixed International Laboratory and LabexMer (ANR-10-LABX-19-01) during her stay at LEMAR for the analyses of DFe samples. Data sets used to generate figures in the manuscript are available at ftp://anonymous@soccohpc.ac.za/Mtshali_etal_2019/.

- Boyd, P. W., & Doney, S. C. (2002). Modelling regional responses by marine pelagic ecosystems to global climate change. *Geophysical Research Letters*, 29(16), 1806. <https://doi.org/10.1029/2001GL014130>
- Boyd, P. W., & Ellwood, M. J. (2010). The biogeochemical cycle of iron in the ocean. *Nature Geoscience*, 3, 675–682. <https://doi.org/10.1038/ngeo964>
- Boyd, P. W., Ellwood, M. J., Tagliabue, A., & Twining, B. S. (2017). Biotic and abiotic retention, recycling and remineralization of metals in the ocean. *Nature Geoscience*, 10, 167–173.
- Boyd, P. W., Ibanami, E., Sander, S. G., Hunter, K. A., & Jackson, G. A. (2010). Remineralization of upper ocean particles: Implications for iron biogeochemistry. *Limnology and Oceanography*, 55(3), 1271–1288. <https://doi.org/10.4319/lo.2010.55.3.1271>
- Boyd, P. W., Law, C. S., Hutchins, D. A., Abraham, E. R., Croot, P. L., Ellwood, M., et al. (2005). FeCycle: Attempting an iron biogeochemical budget from a mesoscale SF6 tracer experiment in unperturbed low iron waters. *Global Biogeochemical Cycles*, 19, GB4S20. <https://doi.org/10.1029/2005GB002494>
- Boyd, P. W., Strzepek, R., Fu, F. X., & Hutchins, D. A. (2010). Environmental control of open-ocean phytoplankton groups: Now and in the future. *Limnology and Oceanography*, 55(3), 1353–1376. <https://doi.org/10.4319/lo.2010.55.3.1353>
- Boye, M., Wake, B. D., Lopez Garcia, P., Bown, J., Baker, A. R., & Achterberg, E. P. (2012). Distributions of dissolved trace metals (Cd, Cu, Mn, Pb, Ag) in the southeastern Atlantic and the Southern Ocean. *Biogeosciences*, 9, 3231–3246. <https://doi.org/10.5194/bg-9-3231-2012>
- Carranza, M. M., & Gille, S. T. (2015). Southern Ocean wind-driven entrainment enhances satellite chlorophyll-a through the summer. *Journal of Geophysical Research: Oceans*, 120, 304–323. <https://doi.org/10.1002/2014JC010203>
- Chever, F., Bucciarelli, E., Sarthou, G., Speich, S., Arhan, M., Penven, P., & Tagliabue, A. (2010). Physical speciation of iron in the Atlantic sector of the Southern Ocean along a transect from the subtropical domain to the Weddell Sea Gyre. *Journal of Geophysical Research*, 115, C10059. <https://doi.org/10.1029/2009JC005880>
- Chever, F., Sarthou, G., Bucciarelli, E., Blain, S., & Bowie, A. R. (2010). An iron budget during the natural iron fertilisation experiment KEOPS (Kerguelen Islands, Southern Ocean). *Biogeosciences*, 7(2), 455–468. <https://doi.org/10.5194/bg-7-455-2010>
- Cutter, G., Casciotti, K. L., Croot, P., Geibert, W., Heimbürger, L., Lohan, M. C., et al. (2013). *Sampling and sample-handling protocols for GEOTRACES cruises*. Toulouse, France: GEOTRACES Standards and Intercalibration Committee.
- de Boyer Montégut, C., Madec, G., Fischer, A. S., Lazar, A., & Iudicone, D. (2004). Mixed layer depth over the global ocean: An examination of profile data and a profile-based climatology. *Journal of Geophysical Research*, 109, C12003. <https://doi.org/10.1029/2004JC002378>
- Egan, L. (2008). *QuickChem Method 31-107-04-1-C - Nitrate and/or Nitrite in Brackish or Seawater*. Colorado, USA: Lachat Instruments.
- Ellwood, M. J., Boyd, P. W., & Sutton, P. (2008). Winter-time dissolved iron and nutrient distributions in the Subantarctic Zone from 40–52S; 155–160E. *Geophysical Research Letters*, 35, L11604. <https://doi.org/10.1029/2008GL033699>
- Fauchereau, N., Tagliabue, A., Bopp, L., & Monteiro, P. M. S. (2011). The response of phytoplankton biomass to transient mixing events in the Southern Ocean. *Geophysical Research Letters*, 38, L17601. <https://doi.org/10.1029/2011GL048498>
- Frew, R. D., Hutchins, D. A., Nodder, S., Sanudo-Wilhelmy, S., Tovar-Sanchez, A., Leblanc, K., et al. (2006). Particulate iron dynamics during FeCycle in sub-Antarctic waters southeast of New Zealand. *Global Biogeochemical Cycles*, 20, GB1S93. <https://doi.org/10.1029/2005GB002558>
- Fung, I. Y., Meyn, S. K., Tegen, I., Doney, S. C., John, J. G., & Bishop, J. K. B. (2000). Iron supply and demand in the upper ocean. *Global Biogeochemical Cycles*, 14(1), 281–295. <https://doi.org/10.1029/1999GB900059>
- Geider, R., & La Roche, J. (2002). Redfield revisited: Variability of C:N:P in marine microalgae and its biochemical basis. *European Journal of Phycology*, 37(1), 1–17. <https://doi.org/10.1017/S0967026201003456>
- Jickells, T. D., An, Z. S., Andersen, K. K., Baker, A. R., Bergametti, G., Brooks, N., et al. (2005). Global iron connection between desert dust, ocean biogeochemistry, and climate. *Science*, 308(5718), 67–71. <https://doi.org/10.1126/science.1105959>
- Joubert, W. R., Thomalla, S. J., Waldron, H. N., Lucas, M. I., Boye, M., Le Moigne, F. A. C., et al. (2011). Nitrogen uptake by phytoplankton in the Atlantic sector of the Southern Ocean during late austral summer. *Biogeosciences*, 8(10), 2947–2959. <https://doi.org/10.5194/bg-8-2947-2011>
- Klunder, M. B., Laan, P., de Baar, H. J. W., & van Oijen, J. C. (2011). Dissolved iron in the Southern Ocean (Atlantic sector). *Deep Sea Research, Part II*, 58, 2678–2694. <https://doi.org/10.1016/j.dsr2.2010.10.042>
- Lancelot, C., de Montety, A., Goosse, H., Becquevort, S., Schoemann, V., Pasquer, B., et al. (2009). Spatial distribution of the iron supply to phytoplankton in the Southern Ocean. a model study. *Biogeosciences*, 6, 2861–2878. <https://doi.org/10.5194/bg-6-2861-2009>
- Law, C. S., Abraham, E. R., Watson, A. J., & Liddicoat, M. I. (2003). Vertical eddy diffusion and nutrient supply to the surface mixed layer of the Antarctic Circumpolar Current. *Journal of Geophysical Research*, 108(C8), 3272. <https://doi.org/10.1029/2002JC001604>
- Mawji, E., Schlitzer, R., Dodas, E. M., Abadie, C., Abouchami, W., Anderson, R. F., et al. (2015). The GEOTRACES intermediate data product 2014. *Marine Chemistry*, 177, 1–8. <https://doi.org/10.1016/j.marchem.2015.04.005>
- Nicholson, S.-A., Lévy, M., Llort, J., Swart, S., & Monteiro, P. M. S. (2016). Investigation into the impact of storms on sustaining summer primary productivity in the Sub-Antarctic Ocean. *Geophysical Research Letters*, 43, 9192–9199. <https://doi.org/10.1002/2016GL069973>
- Obata, H., Karatani, H., & Nakayama, E. (1993). Automated determination of iron in seawater by chelating resin concentration and chemiluminescence detection. *Analytical Chemistry*, 65(11), 1524–1528. <https://doi.org/10.1021/ac00059a007>
- Piola, A. R., & Gordon, A. L. (1989). Intermediate waters in the southwest South Atlantic. *Deep Sea Research*, 36, 1–16.
- Planquette, H., Stathama, P. J., Fonesb, G. R., Charette, M. A., Moored, C. M., Saltera, I., et al. (2007). Dissolved iron in the vicinity of the Crozet Islands, Southern Ocean. *Deep-Sea Research Part II: Topical Studies in Oceanography*, 54(18–20), 1999–2019. <https://doi.org/10.1016/j.dsr2.2007.06.019>
- Platt, T., Gallegos, C. L., & Harrison, W. G. (1980). Photoinhibition of photosynthesis in natural assemblages of marine phytoplankton. *Journal of Marine Research*, 38, 687–701.
- Platt, T., & Sathyendranath, S. (1993). Estimators of primary production for interpretation of remotely-sensed data on ocean colour. *Journal of Geophysical Research*, 98, 14,561–14,576. <https://doi.org/10.1029/93JC01001>
- Pollard, R. T., Salter, I., Sanders, R. J., Lucas, M. I., Moore, C. M., Mills, R. A., et al. (2009). Southern Ocean deep-water carbon export enhanced by natural iron fertilization. *Nature*, 457(7229), 577–580. <https://doi.org/10.1038/nature07716>
- Racault, M.-F., Le Quéré, C., Buitenhuis, E., Sathyendranath, S., & Platt, T. (2012). Phytoplankton phenology in the global ocean. *Ecological Indicators*, 14(1), 152–163. <https://doi.org/10.1016/j.ecolind.2011.07.010>
- Rio, M. H., Guinehut, S., & Larnicol, G. (2011). New CNES-CLS09 global mean dynamic topography computed from the combination of GRACE data, altimetry, and in situ measurements. *Journal of Geophysical Research*, 116, C07018. <https://doi.org/10.1029/2010JC006505>
- Ryan-Keogh, T. J., Thomalla, S. J., Little, H., & Melanson, J.-R. (2018). Seasonal regulation of the coupling of photosynthetic electron transport and carbon fixation in the Southern Ocean. *Limnology and Oceanography*. <https://doi.org/10.1002/lno.10812>

- Ryan-Keogh, T. J., Thomalla, S. J., Mtshali, T. N., & Little, H. (2017). Modelled estimates of spatial variability of iron stress in the Atlantic sector of the Southern Ocean. *Biogeosciences*, *14*(17), 3883–3897. <https://doi.org/10.5194/bg-14-3883-2017>
- Ryan-Keogh, T. J., Thomalla, S. J., Mtshali, T. N., van Horsten, N. R., & Little, H. (2018). Seasonal development of iron limitation in the sub-Antarctic zone. *Biogeosciences*, *15*(14), 4647–4660. <https://doi.org/10.5194/bg-15-4647-2018>
- Sarthou, G., Baker, A. R., Blain, S., Achterberg, E. P., Boye, M., Bowie, A. R., et al. (2003). Atmospheric iron deposition and sea-surface dissolved iron concentrations in the eastern Atlantic Ocean. *Deep Sea Research Part I: Oceanographic Research Papers*, *50*(10–11), 1339–1352. [https://doi.org/10.1016/S0967-0637\(03\)00126-2](https://doi.org/10.1016/S0967-0637(03)00126-2)
- Sarthou, G., Vincent, D., Christaki, U., Obernosterer, I., Timmermans, K. R., & Brussaard, C. P. D. (2008). The fate of biogenic iron during a phytoplankton bloom induced by natural fertilisation: Impact of copepod grazing. *Deep Sea Research, Part II*, *55*(5–7), 734–751. <https://doi.org/10.1016/j.dsr2.2007.12.033>
- Schlitzer, R., Anderson, R. F., Dodas, E. M., Lohan, M., Geibert, W., Tagliabue, A., et al. (2018). The GEOTRACES intermediate data product 2017. *Chemical Geology*, *493*, 210–223. <https://doi.org/10.1016/J.ChemGeo.2018.05.040>
- Sohrin, Y., Iwamoto, S., Matsui, M., Obata, H., Nakayama, E., Suzuki, K., et al. (2000). The distribution of Fe in the Australian sector of the Southern Ocean. *Deep Sea Research Part I: Oceanographic Research Papers*, *47*, 55–84. [https://doi.org/10.1016/S0967-0637\(99\)00049-7](https://doi.org/10.1016/S0967-0637(99)00049-7)
- Strzepek, R. F., Hunter, K. A., Frew, R. D., Harrison, P. J., & Boyd, P. W. (2012). Iron-light interactions differ in Southern Ocean phytoplankton. *Limnology and Oceanography*, *57*(4), 1182–1200. <https://doi.org/10.4319/lo.2012.57.4.1182>
- Strzepek, R. F., Maldonado, M. T., Higgins, J. L., Hall, J., Safi, K., Wilhelm, S. W., & Boyd, P. W. (2005). Spinning the “Ferrous Wheel”: The importance of the microbial community in an iron budget during the FeCycle experiment. *Global Biogeochemical Cycles*, *19*, GB4S26. <https://doi.org/10.1029/2005GB002490>
- Strzepek, R. F., Maldonado, M. T., Hunter, K. A., Frew, R. D., & Boyd, P. W. (2011). Adaptive strategies by Southern Ocean phytoplankton to lessen iron limitation: Uptake of organically complexed iron and reduced cellular iron requirements. *Limnology and Oceanography*, *56*(6), 1983–2002. <https://doi.org/10.4319/lo.2011.56.6.1983>
- Sunda, W. G., & Huntsman, S. A. (1997). Interrelated influence of iron, light and cell size on marine phytoplankton growth. *Nature*, *390*(6658), 389–392. <https://doi.org/10.1038/37093>
- Swart, S., Chang, N., Fauchereau, N., Joubert, W., Lucas, M., Mtshali, T., et al. (2012). Southern Ocean Seasonal Cycle Experiment 2012: Southern scale climate and carbon cycle links. *South African Journal of Science*, *108*(3/4), 11–13. <https://doi.org/10.4102/sajs.v108i3/4.1089>
- Swart, S., Speich, S., Ansoorge, I. J., & Lutjeharms, J. R. E. (2010). An altimetry-based gravest empirical mode south of Africa: 1. Development and validation. *Journal of Geophysical Research*, *115*, C03002. <https://doi.org/10.1029/2009JC005299>
- Swart, S., Thomalla, S. J., & Monteiro, P. M. S. (2015). The seasonal cycle of mixed layer dynamics and phytoplankton biomass in the Sub-Antarctic Zone: A high-resolution glider experiment. *Journal of Marine Systems*, *147*, 103–115. <https://doi.org/10.1016/j.jmarsys.2014.06.002>
- Tagliabue, A., Bopp, L., Dutay, J. C., Bowie, A. R., Chever, F., Jean-Baptiste, P., et al. (2010). Hydrothermal contribution to the oceanic dissolved iron inventory. *Nature Geoscience*, *3*(4), 252–256. <https://doi.org/10.1038/ngeo818>
- Tagliabue, A., Mtshali, T., Aumont, O., Bowie, A. R., Klunder, M. B., Roychoudhury, A. N., & Swart, S. (2012). A global compilation of dissolved iron measurements: focus on distributions and processes in the Southern Ocean. *Biogeosciences*, *9*(6), 2333–2349. <https://doi.org/10.5194/bg-9-2333-2012>
- Tagliabue, A., Sallée, J.-B., Bowie, A. R., Lévy, M., Swart, S., & Boyd, P. W. (2014). Surface-water iron supplies in the Southern Ocean sustained by deep winter mixing. *Nature Geoscience*, *7*(4), 314–320. <https://doi.org/10.1038/ngeo2101>
- Thomalla, S. J., Fauchereau, N., Swart, S., & Monteiro, P. M. S. (2011). Regional scale characteristics of the seasonal cycle of chlorophyll in the Southern Ocean. *Biogeosciences*, *8*(10), 2849–2866. <https://doi.org/10.5194/bg-8-2849-2011>
- Thomalla, S. J., Moutier, W., Ryan-Keogh, T. J., Gregor, L., & Schütt, J. (2017). An optimized method for correcting fluorescence quenching using optical backscattering on autonomous platforms. *Limnology and Oceanography: Methods*, *16*(2), 132–144. <https://doi.org/10.1002/lom3.10324>
- Thomalla, S. J., Ogunkoya, A. G., Vichi, M., & Swart, S. (2017). Using optical sensors on gliders to estimate phytoplankton carbon concentrations and chlorophyll-to-carbon ratios in the Southern Ocean. *Frontiers in Marine Science*, *4*, 34. <https://doi.org/10.3389/fmars.2017.00034>
- Thomalla, S. J., Racault, M.-F., Swart, S., & Monteiro, P. M. S. (2015). High-resolution view of the spring bloom initiation and net community production in the Subantarctic Southern Ocean using glider data. *ICES Journal of Marine Science*, *72*(6), 1999–2020. <https://doi.org/10.1093/icesjms/fsv105>
- Twining, B. S., Baines, S. B., & Fisher, N. S. (2004). Element stoichiometries of individual plankton cells collected during the Southern Ocean Iron Experiment (SOFEX). *Limnology and Oceanography*, *49*(6), 2115–2128. <https://doi.org/10.4319/lo.2004.49.6.2115>
- Twining, B. S., Baines, S. B., Fisher, N. S., & Landry, M. R. (2004). Cellular iron contents of plankton during the Southern Ocean Iron Experiment (SOFEX). *Deep Sea Research, Part I*, *51*(12), 1827–1850. <https://doi.org/10.1016/j.dsr.2004.08.007>
- Wolters, M. (2002). *Determination of silicate in brackish or seawater by flow injection analysis*. *Quikchem Method*, 31–114–27–1–D (p. 12). Loveland, CO: Lachat Instruments.

References from the supporting information

- Atkinson, K. E. (1989). *An introduction to numerical analysis*, (2nd ed.). New York: John Wiley & Sons.